Frontiers in Bioscience Landmark

Front. Biosci. (Landmark Ed) **2026**; 31(3): 47218
https://doi.org/10.31083/FBL47218

Original Research

The Action Mechanism of *Dendrobium* spp. in Treating Dry Eye Disease Based on Network Pharmacology and *In Vitro* Experiments

Shanshan Zhu[1,2,†], Jiayi Li[1,2,†], Yao Lu[1,2], Cheng Sun[1,2], Yushan Zou[1,2], Yujie Wang[1,2], Siqi Wu[1,2], Jin Yao[1,2,*], Wen Bai[1,2,*]

[1]The Affiliated Eye Hospital, Nanjing Medical University, 210029 Nanjing, Jiangsu, China
[2]The Fourth School of Clinical Medicine, Nanjing Medical University, 211166 Nanjing, Jiangsu, China
*Correspondence: yaojin@njmu.edu.cn (Jin Yao); mubaiwen@163.com (Wen Bai)
[†]These authors contributed equally.
Academic Editor: Dario Rusciano
Submitted: 10 October 2025 Revised: 29 January 2026 Accepted: 6 February 2026 Published: 18 March 2026

Abstract

Background: *Dendrobium* spp. has traditionally been used to improve visual function, and related formulations, such as Dendrobium Glow in dark pills, are currently used in the management of dry eye disease (DED). This study investigated the positive effects and underlying mechanisms of 3-O-methylgigantol, an active compound from *Dendrobium* spp., against DED using network pharmacology and *in vitro* experimental validation. **Methods**: Active compounds and targets were identified through database screening, and network analysis was used to identify the key compounds and targets. Molecular docking and dynamic simulations were performed to verify the binding of 3-O-methylgigantol to the epidermal growth factor receptor (EGFR). An *in vitro* DED model was established using hyperosmotic sodium chloride (550 mOsm) in human corneal epithelial cells (HCECs). The effects of 3-O-methylgigantol, with or without the EGFR inhibitor (erlotinib), on cell viability, apoptosis, reactive oxygen species, and inflammatory cytokines were assessed. **Results**: Network pharmacology predicted 3-O-methylgigantol as a key active compound and EGFR as a core target. Molecular simulations confirmed stable binding. *In vitro* experiments showed that 3-O-methylgigantol significantly increased HCEC viability and reduced apoptosis, reactive oxygen species accumulation, and inflammatory cytokine release under hyperosmotic conditions. The EGFR inhibitor erlotinib attenuated these protective effects. **Conclusions**: 3-O-methylgigantol, an active compound from *Dendrobium* spp., alleviates hyperosmolarity-induced corneal epithelial cell damage, oxidative stress, and inflammation by activating the EGFR signaling pathway. This compound may represent a potential therapeutic candidate for DED management, demonstrating its efficacy in restoring tear film homeostasis in *in vitro* models.

Keywords: *Dendrobium* spp.; traditional Chinese medicine; 3-O-methylgigantol; dry eye; network pharmacology

1. Introduction

Dry eye disease (DED) is a multifactorial ocular surface disorder primarily characterized by the loss of tear film homeostasis. It is accompanied by a range of ocular symptoms, including dryness, burning, stinging, foreign body sensation, fluctuating vision, and photophobia, among others [1]. Severe cases may result in loss [2]. With the shift toward modern lifestyles, including the prolonged use of video display terminals and smartphones, the prevalence of DED has increased, posing a growing public health concern and economic burden [3].

Hyperosmolarity of the tear film and ocular surface inflammation are considered core pathological mechanisms underlying DED [3,4]. Hyperosmolarity can directly damage epithelial cells on the ocular surface or indirectly cause harm by inducing inflammatory responses. This inflammatory response involves immune cell infiltration and release of proinflammatory cytokines, chemokines, and matrix metalloproteinases (MMPs), particularly MMP-9 [5]. These factors act synergistically on the ocular surface and the lacrimal glands, leading to tissue damage and functional impairment [6]. Damage and inflammation mutually reinforce each other, creating a “vicious cycle” that results in a chronic progressive disease course [7]. Current therapeutic approaches for DED aim to alleviate symptoms, restore ocular surface homeostasis, and interrupt this vicious cycle [8,9]. Artificial tears typically provide only temporary relief and have low bioavailability [10], resulting in limited efficacy for moderate-to-severe DED. Anti-inflammatory drugs such as cyclosporine and corticosteroids may cause side effects, including increased intraocular pressure and corneal toxicity, with long-term use [11,12]. Emerging therapies, such as secretagogues [13] and local androgens [14,15], are still under investigation [16]. Therefore, developing new safe and effective treatments that target multiple pathological mechanisms, particularly active compounds derived from natural products, has significant clinical potential.

Dendrobium (*Dendrobium* spp.) refers to a group of plants in the Orchidaceae family with medicinal value [17]. It was first documented in *Shennong Bencao Jing* (The Classic of Herbal Medicine), in which it was classified as a

superior herb. According to Traditional Chinese Medicine, *Dendrobium* is believed to nourish the yin, clear heat, benefit the stomach, generate fluids, and improve vision [18]. It is commonly used to treat conditions related to "yin deficiency", such as heat disorders, dry mouth and thirst, insufficient stomach yin, and blurred vision. Notably, traditional uses of *Dendrobium* specifically highlight its "vision-enhancing" or eyesight-improving effects. Among its formulations, Dendrobium Glow in dark pills is widely used to treat DED [19]. Modern phytochemical studies have revealed that *Dendrobium* contains a variety of bioactive compounds, including polysaccharides, alkaloids, bibenzyls [20], phenanthrenes [21], sesquiterpenes, flavonoids, and phenolic compounds [22]. These components contribute to *Dendrobium*'s broad pharmacological activities and may modulate multiple pathogenic pathways [23,24], showing promise as potential therapeutic agents for DED.

Network pharmacology integrates high-throughput omics data, bioinformatics, and network analysis techniques. Its core concept is to analyze the complex interactions between drugs, especially multicomponent drugs, and the body or diseases at the system level within the framework of biological networks. This approach is particularly well-suited for studying traditional Chinese medicine (TCM) formulas, which often involve multiple components, targets, and pathways [25]. The primary objective of this study was to combine network pharmacology and *in vitro* modeling to elucidate the tear film–stabilizing effects of 3-O-methylgigantol, a key phytochemical found in *Dendrobium*, for the treatment of DED.

2. Materials and Methods

2.1 Screening of Active Compounds and Their Targets in Dendrobium

The Encyclopedia of Traditional Chinese Medicine (ETCM) database [26] (http://www.tcmip.cn/ETCM/), HERB database [27] (http://herb.ac.cn/), and relevant literature [28,29] were used to identify the active components of *Dendrobium*. The structures and SMILES identifiers were retrieved from the PubChem database [30] (https://pubchem.ncbi.nlm.nih.gov/). Active compounds were further filtered using the SwissADME database [31] (https://www.swissadme.ch/) by applying the criteria of high gastrointestinal absorption (GI absorption) and drug-likeness, defined by satisfying at least two of the five established rules (Lipinski, Ghose, Veber, Egan, and Muegge) to obtain relevant pharmacologically active compounds [32,33].

The potential *Dendrobium* bioactive compound targets were identified through consensus predictions across multiple databases, including SwissTargetPrediction [34] (https://www.swisstargetprediction.ch/), TargetNet [35] (http://targetnet.scbdd.com/), and Super-PRED [36] (https://prediction.charite.de/). Targets with probability scores exceeding 50% were further validated using the UniProt database [37] (https://www.uniprot.org/), retaining only human protein-coding genes. After deduplication, a curated set of potential *Dendrobium* targets was established for subsequent mechanistic analyses.

2.2 Identification of Potential Dendrobium Targets for Treating Dry Eye

Relevant targets were obtained from the GeneCards database [38] (https://www.genecards.org/Search/) by searching for the keywords "Dry Eye" and "keratoconjunctivitis sicca". Genes with a score of >10 were standardized using the UniProt database [37] and selected as potential therapeutic targets for DED. The intersection of these targets with the potential targets of *Dendrobium*'s active compounds was analyzed to identify possible *Dendrobium* targets for treating DED.

2.3 Construction of the Dendrobium Active Compound-Target Network and Key Node Analysis

A high-confidence interaction score threshold ("High Confidence >0.7") was established, and the target protein interaction data were imported into Cytoscape software (version 3.10.3; Cytoscape Consortium, San Diego, CA, USA) to construct the *Dendrobium* active compound–potential therapeutic target network. The CytoNCA plugin was used to identify key active compounds and critical targets based on node degree and betweenness centrality parameters. The top ten results from both the degree and betweenness centrality analyses were intersected to determine the most important active compounds and targets.

2.4 Functional and Pathway Enrichment Analysis

We used the Enrichr platform (https://maayanlab.cloud/Enrichr/) [39] to perform a biological function analysis of the targets involved in *Dendrobium* treatment of DED using Gene Ontology Biological Process (GO_BP) terms. Pathway analysis was conducted using the MSigDB Hallmark gene sets.

2.5 Molecular Docking and Simulation

Molecular docking between the protein and small-molecule compounds was performed using the Discovery Studio software (version 2019; Dassault Systèmes Biovia, San Diego, CA, USA). The protein-ligand complex then underwent a 100-nanosecond molecular dynamics simulation using GROMACS 2022. CHARMM36 and GAFF2 force fields were used to parameterize the protein and ligand, respectively. The system was solvated with explicit TIP3P water molecules in a cubic periodic box with a 1.2 nm boundary, using the Particle Mesh Ewald method for long-range electrostatics and the Verlet cutoff scheme. Energy minimization was conducted prior to the production runs under NPT ensemble conditions. The system was equilibrated with 100,000 steps each of NVT and NPT simulations (τ = 0.1 ps, duration = 100 ps per equilibration). Van

der Waals and Coulomb interactions were treated with a 1.0 nm cutoff. Production molecular dynamics simulations were performed for 100 ns using GROMACS software (version 2022; Science for Life Laboratory, Stockholm, Sweden), followed by MM/PBSA binding free-energy calculations at equilibrium.

2.6 Cell Line and Treatment

SV40-immortalized human corneal epithelial cells (HCECs, obtained from ATCC CRL-11135) were cultured in DMEM supplemented with 10% FBS (AusGeneX, Molendinar, QLD, Australia; Lot No. FBS500-S) and 1% penicillin/streptomycin (Thermo Fisher Scientific, Inc., Waltham, MA, USA; Cat No. 15140-122) at 37 °C under 5% CO_2. This cell line was validated using STR profiling and tested negative for *Mycoplasma* sp. To simulate hyperosmotic conditions, cells were treated with NaCl to achieve an osmolarity between 312 and 550 mOsm. In some experiments, cells were incubated with 3-O-methylgigantol (0–10 µM) (EvitaChem, Linyi, Shandong, China; Cat No. EVT-8342849) and Erlotinib (0–10 µM) (Selleck Chemicals, Houston, TX, USA; Cat No. S7786).

2.7 Cell Viability Assay

Cell viability was measured using a CCK-8 kit (Biosharp Life Sciences, Hefei, Anhui, China; Cat No. BS350A). Cells were seeded at 1×10^4 cells per well in a 96-well plate and incubated under the respective treatment conditions. Following incubation, CCK-8 solution was added to the wells and incubated at 37 °C for 2 h before measuring absorbance at 450 nm using a Varioskan LUX microplate reader (Thermo Fisher Scientific, Inc., Waltham, MA, USA).

2.8 Detection of Intracellular Reactive Oxygen Species (ROS)

Intracellular ROS levels were measured using 2′,7′-dichlorofluorescin diacetate (DCFH-DA) (Beyotime Institute of Biotechnology, Shanghai, China; Cat No. S0035S). The cells were incubated with 10 µM DCFH-DA at 37 °C for 30 min and observed under a Varioskan LUX microplate reader (Thermo Fisher Scientific, Inc., Waltham, MA, USA). The fluorescence intensity of each cell type was then measured.

2.9 Calcein-AM/PI Staining

Apoptosis was assessed using calcein-AM and propidium iodide (PI) staining. The calcein-AM (Aladdin Biochemical Technology Co., Ltd., Shanghai, China; Cat No. C273362) stock solution contained 1 mM calcein-AM in dimethyl sulfoxide (DMSO). The stock solution was diluted to 1–50 µM with PBS. The stock solution of PI (Solarbio Science & Technology Co., Ltd., Beijing, China; Cat No. C0080) was diluted with PBS to 10–50 µM. The cells were incubated with calcein-AM and PI at room temperature for 15 min and observed under a fluorescence microscope. Calcein-positive cells were considered live, and PI-positive cells were considered apoptotic.

2.10 Enzyme-Linked Immunosorbent Assay (ELISA)

The concentrations of pro-inflammatory cytokines, including interleukin-6 (IL-6), interleukin-1 beta (IL-1β), tumor necrosis factor-alpha (TNF-α), in the cell culture supernatants were determined using commercial Enzyme-Linked Immunosorbent Assay (ELISA) kits (R&D Systems; Bio-Techne, Minneapolis, MN, USA). Specifically, the following kits were employed: IL-6 (Cat No. D6050), IL-1β (Cat No. DLB50), TNF-α (Cat No. DTA00C), and IL-8 (Cat No. D8000C). All procedures were performed strictly according to the manufacturer's instructions. The absorbance was measured at 450 nm using a Varioskan LUX microplate reader (Thermo Fisher Scientific, Inc., Waltham, MA, USA).

2.11 Biotinylation of 3-O-Methylgigantol

Biotinylation of 3-O-methylgigantol was achieved using a two-step click chemistry strategy. First, the alkynyl intermediate was prepared by dissolving 3-O-methylgigantol (1.0 eq) in anhydrous acetone, followed by the addition of anhydrous K_2CO_3 (2.0 eq) as a base. Propargyl bromide (1.2 eq) was added dropwise with stirring, and the mixture was refluxed for 2–4 h. Upon completion, the inorganic salts were filtered, and the filtrate was concentrated under reduced pressure and purified using silica gel column chromatography to yield alkynyl-3-O-methylgigantol. Subsequently, copper-catalyzed azide-alkyne cycloaddition (CuAAC) was performed by co-dissolving the obtained alkynyl intermediate and biotin-azide (1.1 eq) in a DMSO/water mixture (1:1, v/v). $CuSO_4$ (0.1 eq) and sodium ascorbate (0.5 eq) aqueous solutions were added sequentially to generate the catalytic Cu(I) species *in situ*. The reaction mixture was stirred at room temperature in the dark for 1–2 hours. After confirming reaction completion by TLC, the mixture was extracted with ethyl acetate. The crude product was purified by preparative HPLC or column chromatography, then dried under vacuum to yield the final 3-O-methylgigantol-biotin conjugate.

2.12 Small Molecule Pull-Down Assay

A biotin-streptavidin pull-down assay was performed to verify the direct interaction between 3-O-methylgigantol and EGFR. HCECs lysates were prepared in a non-denaturing lysis buffer supplemented with protease and phosphatase inhibitors. Lysates (1 mg protein) were incubated with 20 µM biotin-3-O-methylgigantol overnight at 4 °C. Lysates were pre-incubated with a 10-fold excess (200 µM) of unlabeled 3-O-methylgigantol for 2 h prior to probe addition for competitive inhibition. Biotinylated complexes were captured using Pierce Streptavidin Mag-

netic Beads (Thermo Fisher Scientific, Inc., Waltham, MA, USA; Cat No. 88817) for 2 h at 4 °C. After five washes with lysis buffer, the bound proteins were eluted by heating in sodium dodecyl sulfate (SDS) loading buffer and analyzed by western blotting using a specific anti-EGFR antibody (Cell Signaling Technology, Inc., Danvers, MA, USA; Cat No. 4267; 1:1000 dilution).

2.13 Western Blot

Total protein was extracted from cells using radioimmunoprecipitation assay (RIPA) lysis buffer (Thermo Fisher Scientific, Inc., Waltham, MA, USA; Cat No. 89900) supplemented with protease and phosphatase inhibitor cocktails. The protein concentration was determined using a BCA protein assay kit. Equal amounts of protein (20 µg) were separated by 10% SDS-PAGE and transferred onto PVDF membranes (Millipore). Membranes were blocked with 5% bovine serum albumin (BSA) in TBST for 1 h at room temperature to minimize nonspecific binding. Subsequently, the membranes were incubated overnight at 4 °C with the following primary antibodies from Cell Signaling Technology, Inc. (Danvers, MA, USA): p-EGFR (Tyr1068, #3777; 1:1000), EGFR (#4267; 1:1000), p-AKT (Ser473, #4060; 1:1000), AKT (#4691; 1:1000), and β-Actin (#4970; 1:1000). After washing three times with TBST, the membranes were incubated with HRP-conjugated secondary antibodies (Cell Signaling Technology, Inc., Danvers, MA, USA; #7074; 1:3000) for 1 h at room temperature. Protein bands were visualized using an enhanced chemiluminescence (ECL) detection kit (Thermo Fisher Scientific, Inc., Waltham, MA, USA; Cat No. 34580). The chemiluminescent signals were captured using a ChemiDoc MP Imaging System (Bio-Rad Laboratories, Inc., Hercules, CA, USA). and analyzed using the ImageJ software (version 1.53; National Institutes of Health, Bethesda, MD, USA).

2.14 Statistical Analysis

Study outcomes were quantified using mean $\pm$ standard deviation. The hypothesis testing was conducted in an R computational environment. Comparisons between two groups were conducted using Student's *t*-test using the *t*-test function. Comparisons among multiple groups were performed using one-way analysis of variance (ANOVA) via the aov function, followed by Bonferroni's post-hoc test using the PostHocTest function from the DescTools package. Statistical significance was set at $p < 0.05$.

3. Results

3.1 Active Compounds of Dendrobium

A total of 92 compounds from *Dendrobium* were identified using the ETCM database [26], HERB database [27], and relevant literature [28,29] (Fig. 1A). After screening based on parameters, such as high gastrointestinal absorption and drug-likeness, requiring at least two positive indicators, and supplementation with *Dendrobium* compounds reported in the literature to have high content and pharmacological activity, a total of 43 active compounds were selected (Fig. 1A). The basic information on the active compounds is presented in **Supplementary Table 1**.

3.2 Potential Targets of Dendrobium to Treat DED

The Swiss Target Prediction, Super-PRED, and TargetNet databases were used to predict 909 targets for the 43 active compounds in *Dendrobium* (Fig. 1A). A total of 6787 DED-related therapeutic targets were retrieved from the GeneCards database, and 601 targets with relevance scores greater than 10 were selected as highly associated with DED (Fig. 1A). By intersecting the 909 predicted targets of *Dendrobium* active compounds with 601 DED-related therapeutic targets, 76 common targets were identified. These were considered as potential targets through which *Dendrobium* may exert therapeutic effects on DED (Fig. 1B).

3.3 Network Analysis of Dendrobium Active Compounds and Potential Therapeutic Targets

The top eight key targets based on degree values were APP, AKT1, SRC, EGFR, ESR1, STAT3, ALB, and TNF, which were identified as the primary targets of *Dendrobium* in the treatment of DED (Fig. 1C). Detailed information of the protein-protein interaction (PPI) network is presented in **Supplementary Table 2**. Additionally, a network of *Dendrobium* active compounds and potential therapeutic targets was constructed, and the key interaction data are provided in **Supplementary Table 3**. The top 10 compounds based on intermediate and betweenness centrality (BC) values intersected, yielding four key active compounds: Scoparone, Caffeic acid, 2-Hydroxy-4,7-dimethoxy-9,10-dihydrophenanthrene, and 3-O-methylgigantol, which were considered to be the main active compounds in the treatment of DED (Fig. 1D).

3.4 Functional and Pathway Enrichment Analysis of Dendrobium Targets in the Treatment of DED

Biological functions and pathway predictions for the 76 *Dendrobium* targets for DED treatment were generated using the Enrichr database. MSigDB_Hallmark analysis revealed that these targets were enriched in the PI3K/AKT/mTOR and IL-6/JAK/STAT3 signaling pathways, as well as in apoptotic processes (Fig. 1E). Similarly, Gene Ontology Biological Process analysis indicated enrichment in the activation of cell surface tyrosine kinase signaling and positive regulation of PI3K signaling (Fig. 1F). These analyses allowed us to identify the key biological pathways and molecular mechanisms through which *Dendrobium* may exert therapeutic effects in the treatment of DED.

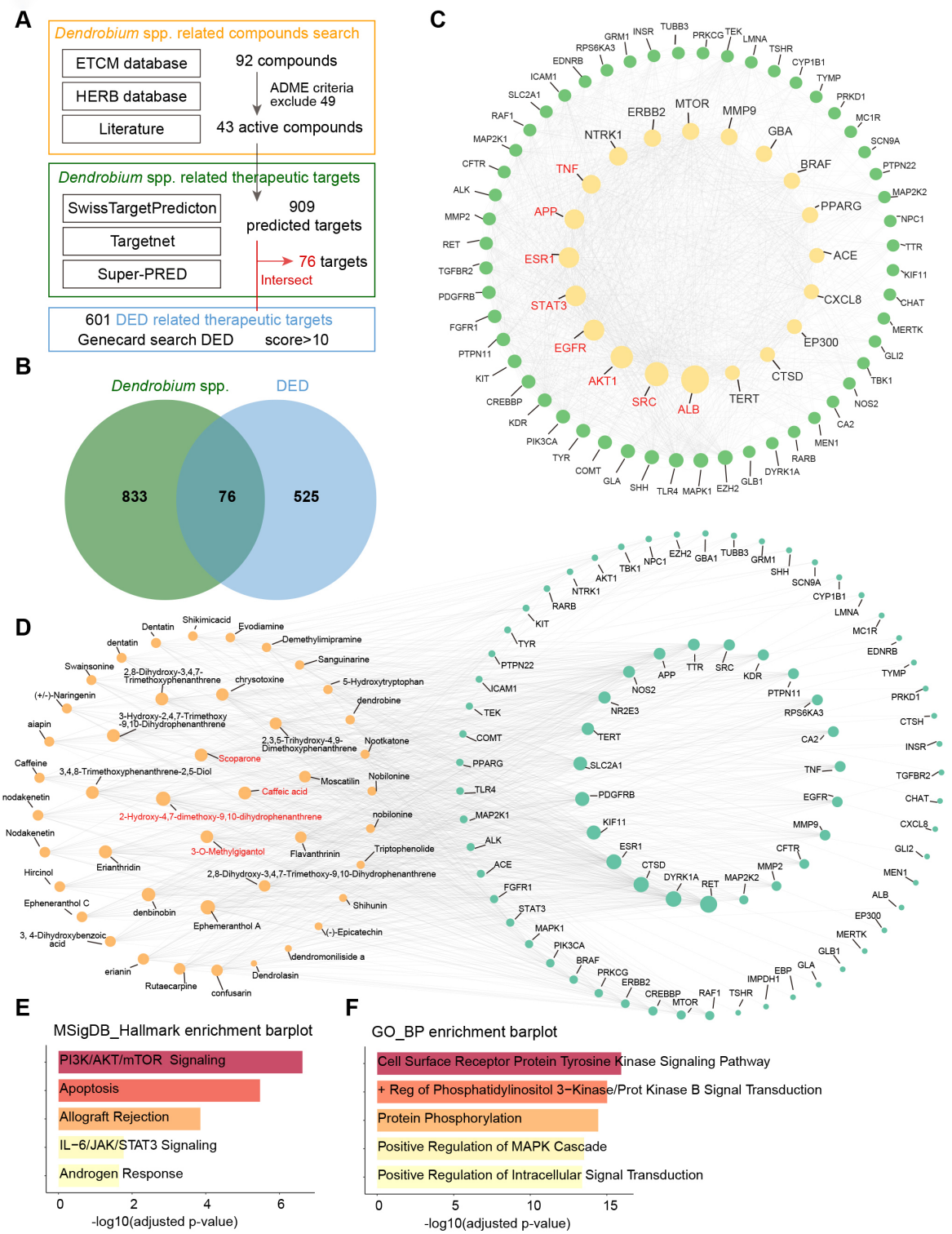

Fig. 1. Network pharmacology analysis of *Dendrobium* in the treatment of dry eye disease (DED). (A) Databases used for screening *Dendrobium* spp.-related and DED-related therapeutic targets. (B) Venn diagram illustrating the intersection (76 common targets) between *Dendrobium* spp.-related targets and DED-related targets, representing potential *Dendrobium* targets for treating DED. (C) The Protein-Protein Interaction (PPI) network of the 76 common targets. The top 8 key therapeutic targets, identified based on degree values, are highlighted in red. (D) The *Dendrobium* active compound-target network. The 4 key active compounds, identified based on degree and betweenness centrality, are highlighted in red. (E,F) Functional and pathway enrichment analyses of the potential targets using Gene Ontology Biological Process (GO_BP) and MSigDB_Hallmarks databases.

3.5 Molecular Docking of Key Active Compounds of Dendrobium With Key Targets

Molecular docking was performed using Discovery Studio to analyze the interactions within the *Dendrobium* active compound–potential therapeutic target network, and the lowest binding affinities were recorded. The results showed that 3-O-methylgigantol exhibited the lowest docking binding affinity with EGFR, at –32.2651 kcal/mol (Fig. 2A). Additionally, the top eight active compound–therapeutic target pairs with the lowest binding affinities were selected for visualization of the molecular docking results (Fig. 2A–H). The binding affinities of these active compounds with their respective targets were all below –5 kcal/mol, indicating that the key active compounds of *Dendrobium* exhibited strong binding affinities to critical targets in DED patients (Fig. 2A–H).

3.6 Molecular Dynamics Simulation of 3-O-Methylgigantol With EGFR

Despite its high centrality across multiple targets, EGFR has been prioritized for molecular dynamics (MD) simulations owing to its biological and physical significance. Biologically, as an upstream cell surface receptor, EGFR initiates intracellular signaling cascades and is a highly accessible target for pharmacological interventions. Physically, it exhibited the lowest binding energy in docking screening, indicating the most stable interaction.

The binding stability of the 3-O-methylgigantol-EGFR complex was investigated using Gromacs, with simulations performed in triplicate. RMSD is a good indicator of the conformational stability of the protein-ligand complex and of the deviation of atomic positions from their initial positions. Lower RMSD values signified restricted backbone fluctuations, reflecting persistent ligand-binding positions. As shown in Fig. 3A, the complex system reached equilibrium after 80 ns, with fluctuations around 2 Å across the three replicates, indicating that the small molecule exhibits high stability upon binding to the target protein.

We used two metrics, the radius of gyration (Rg) and solvent-accessible surface area (SASA), to assess the molecular stability. Rg measures protein compactness and reflects tertiary structure. The SASA quantifies the surface area of a protein that is accessible to the solvent during binding. The SASA is commonly used in simulations to study protein folding, unfolding, and structural stability. Further analysis revealed that the Rg and SASA of the complex remained stable throughout the simulation, indicating that the small molecule–target protein complex did not undergo significant expansion or contraction during movement (Fig. 3B,C). Hydrogen bonds play a crucial role in the binding between the ligand and protein. Fig. 3D shows the number of hydrogen bonds formed between the small molecule and the target protein over time. Throughout the simulation, this count fluctuated between 0 and 4, stabilizing at approximately 2 in most frames, which was consistent across the three replicates. This consistent presence indicated strong hydrogen bonding interactions within the 3-O-methylgigantol-EGFR complex (Fig. 3D).

RMSF quantifies the positional variance in protein residues and maps local flexibility along the polypeptide chain. As shown in Fig. 3E, the RMSF values of the complex are relatively low (mostly below 4 Å), indicating low flexibility and high stability. The RMSF profiles of the three replicates were nearly identical with minor variations across a few regions.

The free energy landscape (FEL) uses a visualization of free energy changes to more intuitively explore the molecular energy landscape and protein-ligand interactions. The energy minima represent stable states, whereas the maxima indicate barriers to conformational change. This method can predict ligand-binding affinities and elucidate molecular recognition mechanisms. In the conformations in which the energy minima occurred in the complex (Fig. 3F–H), van der Waals interactions were formed between the small molecule and the receptor at residues GLY857, ALA763, MET766, LEU777, CYS775, ARG776, CYS797, LEU718, MET793, LEU792, GLY796, THR854, and THR790. Additionally, the receptor residue ASP855 formed a conventional hydrogen bond with small molecules. Furthermore, ASP855 and LYS745 exhibited π-Anion interactions with the small molecule.

Based on the binding conformation of the complex, the binding free energy of 3-O-methylgigantol to EGFR was calculated using MM/PBSA. The binding energies of the three replicates were –12.054, –12.240, and –11.921 kcal/mol, respectively, with a standard deviation of 0.131 kcal/mol. respectively, with a standard deviation of 0.547 kJ/mol. This narrow range underscores the reliability of the calculated binding affinities (Fig. 3I). Further analysis identified key amino acids that contributed significantly to the binding of 3-O-methylgigantol within the complex. Residues ASP855 and LEU788 of EGFR exhibited high contribution values (Fig. 3I), suggesting they may play important roles in the catalytic process.

We monitored the dynamic distances between 3-O-methylgigantol and two key residues to validate the ligand's stability. The hydrogen bond formed between the polar group of the ligand and the acidic side chain of ASP855 remained stable in all three replicate simulations, exhibiting minimal fluctuations throughout the simulations (Fig. 3J). Similarly, the hydrophobic π-alkyl interaction between the ligand's benzene ring and the side chain of LEU788 remained stable, with distances consistently below 5 Å (Fig. 3K). These consistent interactions confirmed the ligands' stable anchoring within the active site.

In conclusion, 3-O-methylgigantol binds stably to EGFR with a low binding free energy, suggesting that it may exert its effects via EGFR.

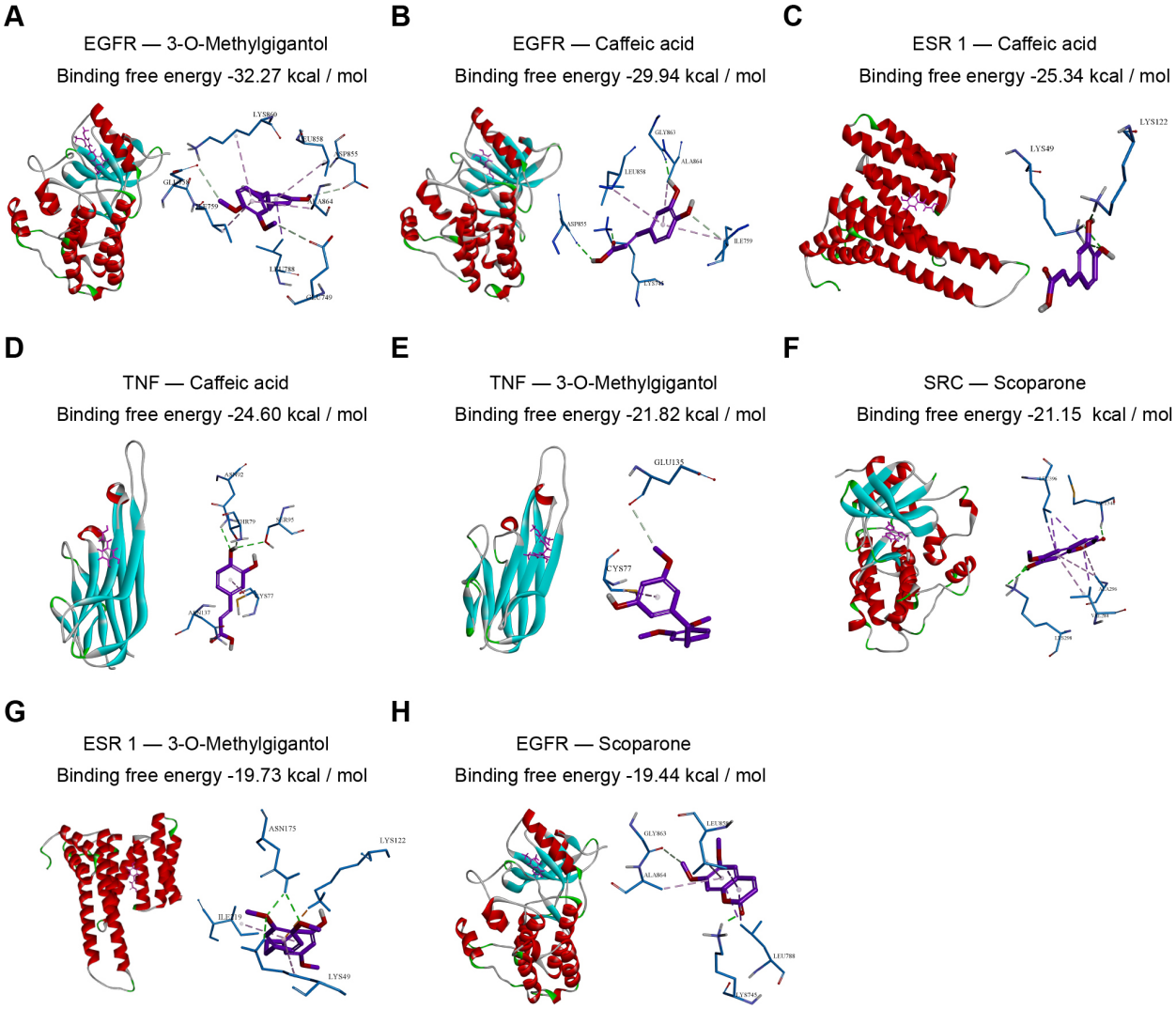

Fig. 2. Molecular docking of key *Dendrobium* active compounds with predicted targets. Molecular docking was performed using Discovery Studio 2019. The figure displays the binding modes and lowest binding energies for the top 8 compound-target pairs, ranked from lowest to highest energy: (A) EGFR – 3-O-methylgigantol, (B) EGFR – Caffeic acid, (C) ESR1 – Caffeic acid, (D) TNF – Caffeic acid, (E) TNF – 3-O-methylgigantol, (F) SRC – Scoparone, (G) ESR1 – 3-O-methylgigantol, and (H) EGFR – Scoparone. Binding affinities less than –5 kcal/mol indicate strong interactions. EGFR, Epidermal Growth Factor Receptor; ESR1, Estrogen Receptor 1; TNF, Tumor Necrosis Factor; SRC, Proto-oncogene Tyrosine-protein Kinase Src.

3.7 3-O-Methylgigantol Targets EGFR and Promotes EGFR Phosphorylation

A 3-O-methylgigantol-biotin conjugate probe (biotin-3-OMG) was synthesized via click chemistry to validate EGFR as a direct target of 3-O-methylgigantol (**Supplementary Fig. 1**). A pull-down assay was performed using a biotinylated probe (biotin-3-OMG). Immunoblotting revealed that biotin-3-OMG significantly enriched EGFR from cell lysates compared to that in the biotin control, indicating a physical interaction (Fig. 3L). Notably, this binding was specific, as it was markedly blocked by preincubation with excess unlabeled 3-OMG (Fig. 3L). Furthermore, 3-OMG treatment significantly upregulated EGFR phosphorylation (p-EGFR, Tyr1068) (Fig. 3L). Collectively, these findings demonstrate that 3-O-methylgigantol directly binds to EGFR and induces its activation.

3.8 3-O-Methylgigantol Inhibits Hypertonic-Induced Epithelial Cell Damage and Inflammation by EGFR Activation

Cell viability of human corneal epithelial cells (HCECs) treated with varying concentrations of hypertonic solutions was assessed using the CCK-8 assay to determine the optimal concentration. In our hypertonic stress experiment, after 24 h of incubation, cell viability decreased in a dose-dependent manner as the osmotic pressure increased from 312 to 550 mOsm (**Supplementary Fig. 2**). When the

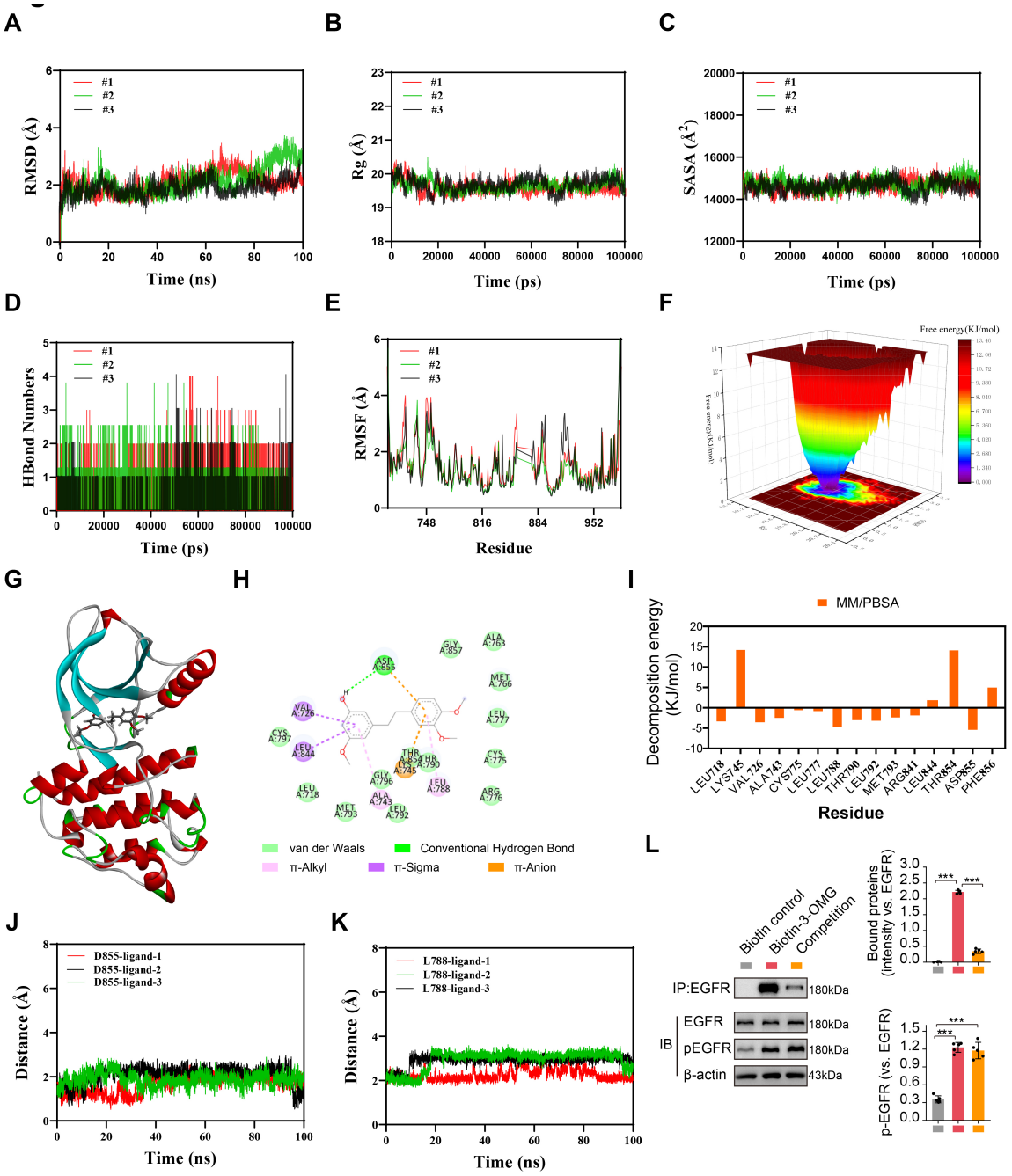

Fig. 3. Molecular dynamics (MD) simulation and validation of the 3-O-methylgigantol–EGFR interaction. A 100 ns MD simulation was conducted using Gromacs 2022 in three independent replicates. Analysis included: (A) RMSD. (B) Radius of Gyration (Rg). (C) SASA. (D) Number of hydrogen bonds. (E) RMSF. (F) Free Energy Landscape (FEL) profile. (G) 3D and (H) 2D representations of the complex conformation at the minimum binding free energy. (I) MM/PBSA analysis identifying key amino acid residues contributing to the binding free energy. (J,K) The distances between 3-O-methylgigantol and the ASP855 (J) and LEU788 (K) residues within the EGFR active site. (L) HCEC cell lysates were incubated with biotinylated 3-OMG (Biotin-3-OMG) or biotin control, followed by precipitation with streptavidin-conjugated beads. For the competition group, lysates were pre-incubated with an excess of unlabeled 3-OMG prior to the addition of Biotin-3-OMG. The presence of EGFR in the pull-down precipitates was detected by immunoblotting. Phosphorylation levels of EGFR (Tyr1068) and total EGFR were analyzed by Western blotting. Data are presented as means ± SD. ***$p < 0.001$. Pairwise comparisons were conducted using One-way ANOVA with Bonferroni's post hoc test (L). RMSD, Root Mean Square Deviation; SASA, Solvent-Accessible Surface Area; RMSF, Root Mean Square Fluctuation; MM/PBSA, Molecular Mechanics/Poisson-Boltzmann Surface Area; HCEC, Human Corneal Epithelial Cell; ANOVA, Analysis of Variance.

osmotic pressure reached 550 mOsm, the cell viability declined to approximately 50%; therefore, this concentration was selected for subsequent experiments. Following treatment with different concentrations of 3-O-methylgigantol (312–550 mOsm) for 24 h, the cell viability increased in a dose-dependent manner. At a 5 μM concentration, 3-O-methylgigantol significantly enhanced the cell viability (Fig. 4A) and mitigated the reduction in cell viability induced by hypertonic stress (Fig. 4B).

To determine whether EGFR is a key mediator of 3-O-methylgigantol-induced HCEC activation, we used the EGFR inhibitor, erlotinib. Erlotinib binds to the ATP-binding site, preventing the activation of EGFR kinase by binding to ATP and transferring phosphate groups to substrates. First, to rule out potential off-target cytotoxicity, we evaluated the viability of HCECs treated with a concentration gradient of Erlotinib (0.1, 0.5, 1, 5, and 10 μM) under normal culture conditions. The CCK-8 assay indicated that Erlotinib exhibited no significant toxicity at concentrations up to 5 μM (Fig. 4C). Therefore, we performed dose-dependent blocking assays. Under hypertonic stress, HCECs were co-treated with 5 μM 3-O-methylgigantol and increasing concentrations of Erlotinib (0.1, 1.0, and 5.0 μM). Erlotinib attenuated the protective effect of 3-O-methylgigantol in a dose-dependent manner. While 0.1 μM showed partial inhibition, 5 μM Erlotinib completely abolished the 3-O-methylgigantol-mediated restoration of cell viability and exacerbated hypertonic damage (Fig. 4D). These findings confirm that the protective action of 3-O-methylgigantol is specifically dependent on EGFR signaling activity.

Cell apoptosis was assessed using calcein-AM/PI staining, revealing that 3-O-methylgigantol alleviated hypertonic-induced apoptosis in HCECs, an effect that was blocked by Erlotinib (Fig. 4E). DCFH-DA staining, used to measure intracellular ROS levels, showed that 3-O-methylgigantol reduced hypertonic-induced ROS accumulation in HCECs, and this effect was inhibited by Erlotinib (Fig. 4F). ELISA assays measured the levels of TNF-α, IL-1β, IL-6, and IL-8, which were elevated in HCECs under hypertonic conditions (Fig. 4G–J). Treatment with 3-O-methylgigantol reduced the hypertonicity-induced increase in inflammatory cytokines, an effect blocked by Erlotinib (Fig. 4G–J). Western blotting was performed to elucidate the underlying mechanism. The results indicated that the phosphorylation levels of EGFR and its downstream effector AKT were suppressed under hypertonic conditions (Fig. 4K–M). However, 3-O-methylgigantol treatment restored p-EGFR and p-AKT expression, whereas the addition of Erlotinib abolished this activation (Fig. 4K–M), confirming the dependence of 3-O-methylgigantol on EGFR signal activation. These results suggest that 3-O-methylgigantol acts through EGFR to significantly alleviate epithelial apoptosis, oxidative stress, and inflammation under hypertonic conditions.

4. Discussion

DED is characterized by a tear film imbalance that causes dryness, fatigue, foreign body sensation, and pain. Untreated condition can cause inflammatory damage to the cornea and the conjunctiva. *Dendrobium* exhibits antitumor, immunomodulatory, antioxidant, anti-inflammatory, anti-aging, anti-cataract, and digestion-promoting properties. Recently, its potential for the treatment of DED has gained attention. In a DED rat model, *Dendrobium* water extracts enhanced tear secretion, protected the ocular surface structure, increased goblet cell numbers and mucin expression, and inhibited the activation of MAPK and NF-κB pathways, thereby reducing ocular inflammation [40]. However, the active components of *Dendrobium* and their roles in DED remain unclear.

This study used network pharmacology to identify four key bioactive compounds from *Dendrobium* scoparone, caffeic acid, 2-Hydroxy-4,7-dimethoxy-9,10-dihydrophenanthrene, and 3-O-methylgigantol, considered core agents for the treatment of dry eye syndrome. Scoparone and Caffeic acid exhibit strong anti-inflammatory and immunomodulatory effects by inhibiting the NF-κB pathway and reducing cytokines (e.g., IL-6, TNF-α) [41, 42], making them promising for alleviating ocular surface inflammation in patients with DED. However, limited data are available on the biological activity and pharmacology of 3-O-methylgigantol.

3-O-methylgigantol, which is found in several *Dendrobium* species, including *Dendrobium* fimbriatum, is one of the primary active compounds. Although their specific bioactivity remains underexplored, stilbene analogs possess anti-inflammatory and antioxidant properties. Given that its parent compound, gigantol, exhibits various pharmacological effects, 3-O-methylgigantol is expected to have significant therapeutic potential, particularly in diseases related to inflammation and oxidative stress. To date, no studies have reported the role or mechanism of DED.

Network pharmacology analysis identified EGFR as the principal target. Molecular docking and kinetic simulation validated the stable binding interaction between 3-O-methylgigantol and EGFR. Notably, this receptor is abundantly expressed in corneal epithelial cells. Proper EGFR signaling is crucial for corneal epithelial homeostasis, as it regulates cellular renewal, barrier function, and injury repair. EGFR activation relies on ligands such as epidermal growth factor (EGF), transforming growth factor-alpha (TGF-α), and heparin-binding EGF-like growth factor (HB-EGF), which maintain basal EGFR activity in healthy tear fluid [43]. In DED, reduced EGFR and TGF-α levels impair signaling [44], diminishing activity in key pathways like PI3K/Akt and MAPK/ERK [45]. This weakens cell survival and reparative capacity, compromising the corneal barrier and exacerbating dry eye symptoms. Our network pharmacology study identified 909 potential *Dendrobium* targets, indicating that its protective effects

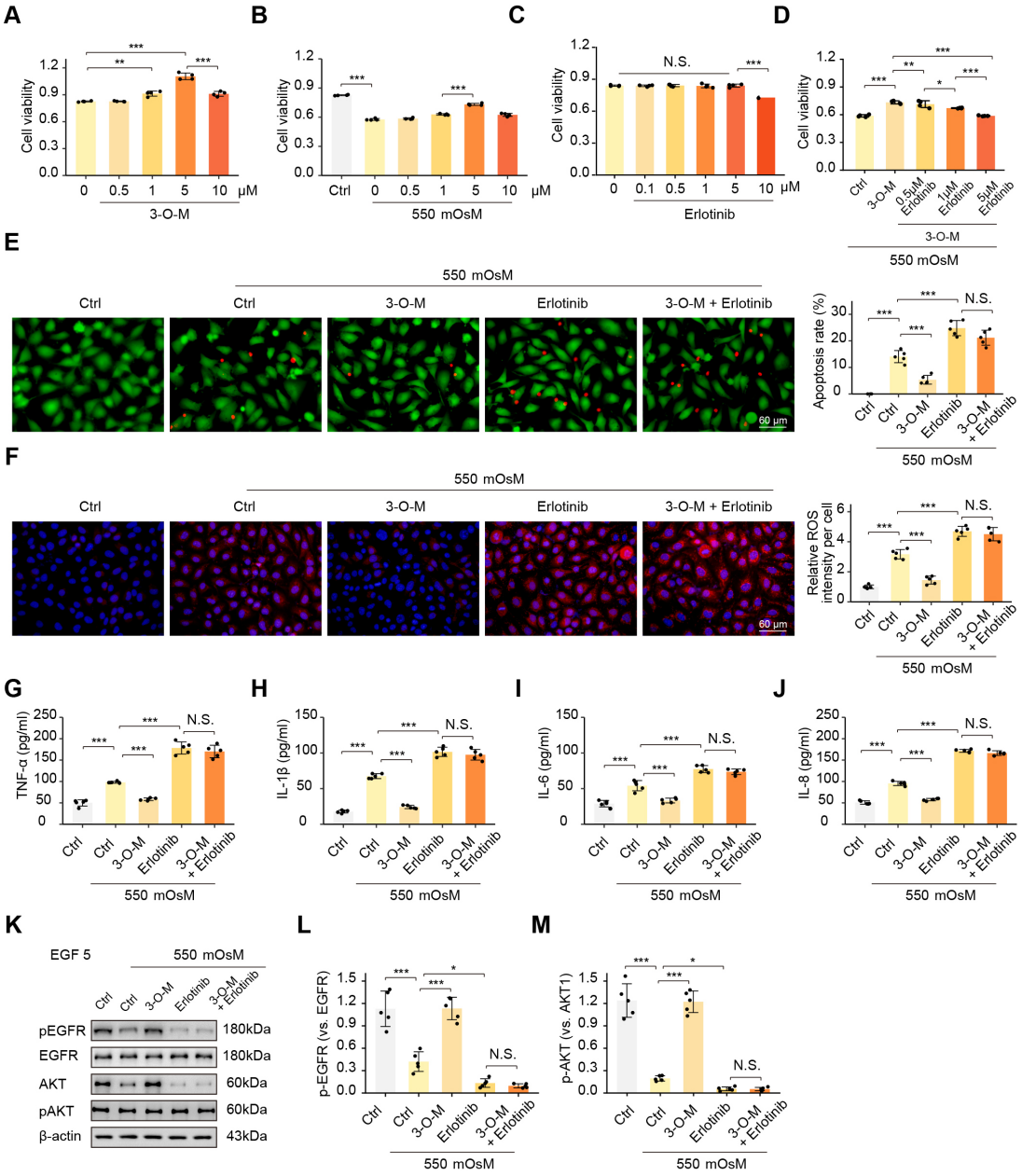

Fig. 4. 3-O-methylgigantol ameliorates hyperosmotic-induced cytotoxicity in HCECs via the EGFR pathway. (A–D) Viability of Human Corneal Epithelial Cells (HCECs) measured by the CCK-8 assay (n = 4 biological repeats): (A) HCECs treated with different concentrations of 3-O-methylgigantol for 24 h under normal conditions. (B) HCECs were treated with different concentrations of 3-O-methylgigantol for 24 h under 550 mOsM hyperosmotic stress. (C) HCECs were treated with different concentrations of the EGFR inhibitor Erlotinib for 24 h under normal conditions. (D) HCECs treated with 5 μM 3-O-methylgigantol alone or combined with different concentrations of Erlotinib for 24 h under 550 mOsM stress. (E–J) HCECs treated with 5 μM 3-O-methylgigantol ± 5 μM Erlotinib under 550 mOsM stress for 24 h (n = 5 biological repeats): (E) Calcein-AM/PI staining for cell apoptosis (Green: live cells, Red: apoptotic cells). Scale bar = 60 μm. (F) DCFH-DA staining for intracellular ROS. Scale bar = 60 μm. (G–J) ELISA measurement of inflammatory cytokines TNF-α, IL-1β, IL-6, and IL-8. (K–M) Western blot analysis of EGFR and AKT phosphorylation. Cells were treated with EGF (100 ng/mL) for 5 min. Representative protein bands and quantification of the p-EGFR/EGFR and p-AKT/AKT ratios. Data are presented as means ± SD. N.S., $p \geq 0.05$; *$p < 0.05$, **$p < 0.01$, ***$p < 0.001$. Pairwise comparisons were conducted using One-way ANOVA with Bonferroni's post hoc test (A–M). CCK-8, Cell Counting Kit-8; DCFH-DA, 2′,7′-dichlorofluorescin diacetate; ROS, Reactive Oxygen Species; ELISA, Enzyme-linked Immunosorbent Assay; TNF-α, Tumor Necrosis Factor-Alpha; IL-1β, Interleukin-1 Beta; IL-6, Interleukin-6; IL-8, Interleukin-8; AKT, AKT serine/threonine kinase; EGF, Epidermal Growth Factor; SD, Standard Deviation.

against dry eye may involve multiple targets, particularly the PI3K/Akt pathway.

Hyperosmolarity of the tear film is the core mechanism of DED [46] and is caused by either insufficient tear secretion or excessive evaporation [47]. It damages the epithelial cells on the ocular surface, triggering oxidative stress, inflammation, and apoptosis [48]. In our *in vitro* hyperosmolarity model, 550 mOsm/L was selected as the optimal concentration to simulate dry eye conditions. We found that 3-O-methylgigantol effectively alleviated corneal epithelial damage caused by hyperosmolarity and reduced reactive oxygen species accumulation and inflammatory cytokine levels. These experiments validate the potential therapeutic role of 3-O-methylgigantol in treating hyperosmotic corneal damage.

5. Limitations

This study has several limitations. First, our investigation relied solely on a single SV40-immortalized HCEC line [49]. Although this cell line serves as a reproducible *in vitro* model, the immortalization processmediated by the SV40 Large T antigen involves the functional inactivation of p53 and retinoblastoma (Rb) tumor suppressor pathways [50]. This mechanism is known to dysregulate cell cycle checkpoints and apoptotic signaling, potentially resulting in inflammatory and survival responses that differ from those observed in primary corneal epithelial cells. Second, the study was conducted exclusively *in vitro* without *in vivo* validation of 3-O-methylgigantol's tear film stabilization or corneal epithelial repair effects. Future studies should verify these findings using established animal models of dry eye to determine the therapeutic dose and confirm the absence of systemic or local adverse effects. Furthermore, small molecules frequently exhibit polypharmacology, including off-target binding, which may lead to unintended cytotoxicity or functional impairment of sensitive ocular tissues. Therefore, comprehensive and unbiased screening, such as high-throughput profiling, is essential to fully map the target profile of a compound and ensure both specificity and long-term safety prior to clinical translation.

6. Conclusions

This study comprehensively explored the therapeutic potential of Dendrobium and its active constituents in the treatment of DED using network pharmacology, molecular docking, and cellular assays. These results suggest that these compounds may protect the ocular surface by modulating inflammation, oxidative stress, and key signaling pathways such as EGFR/PI3K/AKT. Notably, 3-O-methylgigantol, the key focus of this study, was the first compound to alleviate hyperosmolarity-induced corneal epithelial damage via EGFR activation, providing important evidence for novel dry eye treatments.

Abbreviations

DED, Dry Eye Disease; EGF, Epidermal Growth Factor; EGFR, Epidermal Growth Factor Receptor; ERK, Extracellular Signal-Regulated Kinase; HCECs, Human Corneal Epithelial Cells; BC, Betweenness Centrality; TNF-α, Tumor Necrosis Factor-Alpha; IL-1β, Interleukin-1 Beta; IL-6, Interleukin-6; IL-8, Interleukin-8; GO, gene ontology; MD, Molecular Dynamics; MM/PBSA, Molecular Mechanics/Poisson-Boltzmann Surface Area; PPI, Protein-Protein Interaction; FEL, Free Energy Landscape; Rg, Radius of Gyration; RMSD, Root Mean Square Deviation; RMSF, Root Mean Square Fluctuation; ROS, Reactive Oxygen Species; SASA, Solvent-Accessible Surface Area; SD, Standard Deviation.

Availability of Data and Materials

The datasets generated and analyzed during the current study are available from the corresponding author on reasonable request.

Author Contributions

JY and WB designed the research study. SZ, JL, and YL performed the research. CS and YZ conducted the ELISA experiments, contributing substantially to data acquisition. JL analyzed the data. SZ drafted the manuscript. YW and SW visualized the data and prepared the figures. All authors contributed to critical revision of the manuscript for important intellectual content. All authors read and approved the final manuscript. All authors have participated sufficiently in the work and agreed to be accountable for all aspects of the work.

Ethics Approval and Consent to Participate

Not applicable.

Acknowledgment

We thank the medical laboratory of the Eye Hospital, Nanjing Medical University, for providing the experimental equipment and space. We would like to thank Editage for English language editing. The graphical abstract was created in BioRender (https://www.biorender.com/). Yao, L. (2026) https://BioRender.com/xw5gpv9.

Funding

This research received no external funding.

Conflict of Interest

The authors declare no conflict of interest.

Supplementary Material

Supplementary material associated with this article can be found, in the online version, at https://doi.org/10.31083/FBL47218.

References

[1] Zemanová M. DRY EYE DISEASE. A REVIEW. Ceska a Slovenska Oftalmologie: Casopis Ceske Oftalmologicke Spolecnosti a Slovenske Oftalmologicke Spolecnosti. 2021; 77: 107–119. https://doi.org/10.31348/2020/29.

[2] Uchino M, Schaumberg D A. Dry eye disease: impact on quality of life and vision. Current ophthalmology reports. 2013; 1: 51–57. https://doi.org/10.1007/s40135-013-0009-1.

[3] Craig JP, Nelson JD, Azar DT, Belmonte C, Bron AJ, Chauhan SK, *et al*. TFOS DEWS II Report Executive Summary. The Ocular Surface. 2017; 15: 802–812. https://doi.org/10.1016/j.jtos.2017.08.003.

[4] Kang WS, Jung E, Kim J. *Aucuba japonica* Extract and Aucubin Prevent Desiccating Stress-Induced Corneal Epithelial Cell Injury and Improve Tear Secretion in a Mouse Model of Dry Eye Disease. Molecules (Basel, Switzerland). 2018; 23: 2599. https://doi.org/10.3390/molecules23102599.

[5] Yu L, Yu C, Dong H, Mu Y, Zhang R, Zhang Q, *et al*. Recent Developments About the Pathogenesis of Dry Eye Disease: Based on Immune Inflammatory Mechanisms. Frontiers in Pharmacology. 2021; 12: 732887. https://doi.org/10.3389/fphar.2021.732887.

[6] Han Y, Guo S, Li Y, Li J, Zhu L, Liu Y, *et al*. Berberine ameliorate inflammation and apoptosis via modulating PI3K/AKT/NFκB and MAPK pathway on dry eye. Phytomedicine: International Journal of Phytotherapy and Phytopharmacology. 2023; 121: 155081. https://doi.org/10.1016/j.phymed.2023.155081.

[7] Messmer EM, Ahmad S, Benitez Del Castillo JM, Mrukwa-Kominek E, Rolando M, Vitovska O, *et al*. Management of inflammation in dry eye disease: Recommendations from a European panel of experts. European Journal of Ophthalmology. 2023; 33: 1294–1307. https://doi.org/10.1177/11206721221141481.

[8] Periman LM, Perez VL, Saban DR, Lin MC, Neri P. The Immunological Basis of Dry Eye Disease and Current Topical Treatment Options. Journal of Ocular Pharmacology and Therapeutics: the Official Journal of the Association for Ocular Pharmacology and Therapeutics. 2020; 36: 137–146. https://doi.org/10.1089/jop.2019.0060.

[9] Mohamed HB, Abd El-Hamid BN, Fathalla D, Fouad EA. Current trends in pharmaceutical treatment of dry eye disease: A review. European Journal of Pharmaceutical Sciences: Official Journal of the European Federation for Pharmaceutical Sciences. 2022; 175: 106206. https://doi.org/10.1016/j.ejps.2022.106206.

[10] Labetoulle M, Benitez-Del-Castillo JM, Barabino S, Herrero Vanrell R, Daull P, Garrigue JS, *et al*. Artificial Tears: Biological Role of Their Ingredients in the Management of Dry Eye Disease. International Journal of Molecular Sciences. 2022; 23: 2434. https://doi.org/10.3390/ijms23052434.

[11] Liu SH, Saldanha IJ, Abraham AG, Rittiphairoj T, Hauswirth S, Gregory D, *et al*. Topical corticosteroids for dry eye. The Cochrane Database of Systematic Reviews. 2022; 10: CD015070. https://doi.org/10.1002/14651858.CD015070.pub2.

[12] Nagai N, Otake H. Novel drug delivery systems for the management of dry eye. Advanced Drug Delivery Reviews. 2022; 191: 114582. https://doi.org/10.1016/j.addr.2022.114582.

[13] Simsek C, Kojima T, Nakamura S, Dogru M, Tsubota K. The Effects of Rebamipide 2% Ophthalmic Solution Application on Murine Subbasal Corneal Nerves After Environmental Dry Eye Stress. International Journal of Molecular Sciences. 2019; 20: 4031. https://doi.org/10.3390/ijms20164031.

[14] Jiang JR, Khankan R, Ridder WH, 3rd, Paugh JR. Treatment of severe dry eye following acoustic neuroma surgery with eyelid androgen gel application. American Journal of Ophthalmology Case Reports. 2024; 37: 102241. https://doi.org/10.1016/j.ajoc.2024.102241.

[15] Wang LX, Huang LS, Qiu S, Deng YP. Effect of androgen replacement therapy on mixed dry eye in a rabbit model. Zhonghua Yi Xue Za Zhi. 2021; 101: 2525–2530. https://doi.org/10.3760/cma.j.cn112137-20210322-00713.

[16] O'Neil EC, Henderson M, Massaro-Giordano M, Bunya VY. Advances in dry eye disease treatment. Current Opinion in Ophthalmology. 2019; 30: 166–178. https://doi.org/10.1097/ICU.0000000000000569.

[17] Yang J, Kuang MT, Yang L, Huang W, Hu JM. Modern interpretation of the traditional application of Shihu - A comprehensive review on phytochemistry and pharmacology progress of Dendrobium officinale. Journal of Ethnopharmacology. 2023; 302: 115912. https://doi.org/10.1016/j.jep.2022.115912.

[18] Zhang P, Zhang X, Zhu X, Hua Y. Chemical Constituents, Bioactivities, and Pharmacological Mechanisms of *Dendrobium officinale*: A Review of the Past Decade. Journal of Agricultural and Food Chemistry. 2023; 71: 14870–14889. https://doi.org/10.1021/acs.jafc.3c04154.

[19] Wu H, Xu J, Du X, Cui J, Zhang T, Chen Y. Shihu Yeguang Pill protects against bright light-induced photoreceptor degeneration in part through suppressing photoreceptor apoptosis. Biomedicine & Pharmacotherapy = Biomedecine & Pharmacotherapie. 2020; 126: 110050. https://doi.org/10.1016/j.biopha.2020.110050.

[20] He L, Su Q, Bai L, Li M, Liu J, Liu X, *et al*. Recent research progress on natural small molecule bibenzyls and its derivatives in Dendrobium species. European Journal of Medicinal Chemistry. 2020; 204: 112530. https://doi.org/10.1016/j.ejmech.2020.112530.

[21] Sarakulwattana C, Mekboonsonglarp W, Likhitwitayawuid K, Rojsitthisak P, Sritularak B. New bisbibenzyl and phenanthrene derivatives from *Dendrobium scabrilingue* and their α-glucosidase inhibitory activity. Natural Product Research. 2020; 34: 1694–1701. https://doi.org/10.1080/14786419.2018.1527839.

[22] Zhang C, Chen J, Huang W, Song X, Niu J. Transcriptomics and Metabolomics Reveal Purine and Phenylpropanoid Metabolism Response to Drought Stress in *Dendrobium sinense*, an Endemic Orchid Species in Hainan Island. Frontiers in Genetics. 2021; 12: 692702. https://doi.org/10.3389/fgene.2021.692702.

[23] Kongkatitham V, Dehlinger A, Chaotham C, Likhitwitayawuid K, Böttcher C, Sritularak B. Diverse modulatory effects of bibenzyls from Dendrobium species on human immune cell responses under inflammatory conditions. PloS One. 2024; 19: e0292366. https://doi.org/10.1371/journal.pone.0292366.

[24] Wan J, Lin R, Wu Q. The therapeutic effects of dendrobium officinale polysaccharides on diabetes mellitus: from the perspective of gut microbiota. Frontiers in Endocrinology. 2025; 16: 1683752. https://doi.org/10.3389/fendo.2025.1683752.

[25] Zhang RZ, Yu SJ, Bai H, Ning K. TCM-Mesh: The database and analytical system for network pharmacology analysis for TCM preparations. Scientific Reports. 2017; 7: 2821. https://doi.org/10.1038/s41598-017-03039-7.

[26] Xu HY, Zhang YQ, Liu ZM, Chen T, Lv CY, Tang SH, *et al*. ETCM: an encyclopaedia of traditional Chinese medicine. Nucleic Acids Research. 2019; 47: D976–D982. https://doi.org/10.1093/nar/gky987.

[27] Gao K, Liu L, Lei S, Li Z, Huo P, Wang Z, *et al*. HERB 2.0: an updated database integrating clinical and experimental evidence for traditional Chinese medicine. Nucleic Acids Research. 2025; 53: D1404–D1414. https://doi.org/10.1093/nar/gkae1037.

[28] Wei L, Dong W, Han Z, Chen C, Jin Q, He J, *et al*. Network Pharmacologic Analysis of *Dendrobium officinale* Extract Inhibiting the Proliferation of Gastric Cancer Cells. Frontiers in Pharmacology. 2022; 13: 832134. https://doi.org/10.3389/fphar.2022.

832134.
[29] Yao L, Fang J, Zhao J, Yu J, Zhang X, Chen W, *et al*. Dendrobium huoshanense in the treatment of ulcerative colitis: Network pharmacology and experimental validation. Journal of Ethnopharmacology. 2024; 323: 117729. https://doi.org/10.1016/j.jep.2024.117729.
[30] Kim S, Thiessen PA, Bolton EE, Chen J, Fu G, Gindulyte A, *et al*. PubChem Substance and Compound databases. Nucleic Acids Research. 2016; 44: D1202–D1213. https://doi.org/10.1093/nar/gkv951.
[31] Daina A, Michielin O, Zoete V. SwissADME: a free web tool to evaluate pharmacokinetics, drug-likeness and medicinal chemistry friendliness of small molecules. Scientific Reports. 2017; 7: 42717. https://doi.org/10.1038/srep42717.
[32] Liao Q, Guo Z, Ding C, Zuo R, Liu G. Integrating network analysis and experimental validation to reveal the ferroptosis-associated mechanism of velvet antler in the treatment of chronic atrophic gastritis. Journal of Food and Drug Analysis. 2025; 33: 119–131. https://doi.org/10.38212/2224-6614.3546.
[33] Ren J, Dai J, Chen Y, Wang Z, Sha R, Mao J, *et al*. Hypoglycemic Activity of Rice Resistant-Starch Metabolites: A Mechanistic Network Pharmacology and In Vitro Approach. Metabolites. 2024; 14: 224. https://doi.org/10.3390/metabo14040224.
[34] Daina A, Michielin O, Zoete V. SwissTargetPrediction: updated data and new features for efficient prediction of protein targets of small molecules. Nucleic Acids Research. 2019; 47: W357–W364. https://doi.org/10.1093/nar/gkz382.
[35] Yao ZJ, Dong J, Che YJ, Zhu MF, Wen M, Wang NN, *et al*. TargetNet: a web service for predicting potential drug-target interaction profiling via multi-target SAR models. Journal of Computer-aided Molecular Design. 2016; 30: 413–424. https://doi.org/10.1007/s10822-016-9915-2.
[36] Gallo K, Goede A, Preissner R, Gohlke BO. SuperPred 3.0: drug classification and target prediction-a machine learning approach. Nucleic Acids Research. 2022; 50: W726–W731. https://doi.org/10.1093/nar/gkac297.
[37] Apweiler R, Bairoch A, Wu CH, Barker WC, Boeckmann B, Ferro S, *et al*. UniProt: the Universal Protein knowledgebase. Nucleic Acids Research. 2004; 32: D115–D119. https://doi.org/10.1093/nar/gkh131.
[38] Stelzer G, Rosen N, Plaschkes I, Zimmerman S, Twik M, Fishilevich S, *et al*. The GeneCards Suite: From Gene Data Mining to Disease Genome Sequence Analyses. Current Protocols in Bioinformatics. 2016; 54: 1.30.1–1.30.33. https://doi.org/10.1002/cpbi.5.
[39] Kuleshov MV, Jones MR, Rouillard AD, Fernandez NF, Duan Q, Wang Z, *et al*. Enrichr: a comprehensive gene set enrichment analysis web server 2016 update. Nucleic Acids Research. 2016; 44: W90–W97. https://doi.org/10.1093/nar/gkw377.
[40] Ling J, Chan CL, Ho CY, Gao X, Tsang SM, Leung PC, *et al*. The Extracts of Dendrobium Alleviate Dry Eye Disease in Rat Model by Regulating Aquaporin Expression and MAPKs/NF-κB Signalling. International Journal of Molecular Sciences. 2022; 23: 11195. https://doi.org/10.3390/ijms231911195.
[41] Lu C, Li Y, Hu S, Cai Y, Yang Z, Peng K. Scoparone prevents IL-1β-induced inflammatory response in human osteoarthritis chondrocytes through the PI3K/Akt/NF-κB pathway. Biomedicine & Pharmacotherapy = Biomedecine & Pharmacotherapie. 2018; 106: 1169–1174. https://doi.org/10.1016/j.biopha.2018.07.062.
[42] Zhang M, Zhou J, Wang L, Li B, Guo J, Guan X, *et al*. Caffeic acid reduces cutaneous tumor necrosis factor alpha (TNF-α), IL-6 and IL-1β levels and ameliorates skin edema in acute and chronic model of cutaneous inflammation in mice. Biological & Pharmaceutical Bulletin. 2014; 37: 347–354. https://doi.org/10.1248/bpb.b13-00459.
[43] Sabbah DA, Hajjo R, Sweidan K. Review on Epidermal Growth Factor Receptor (EGFR) Structure, Signaling Pathways, Interactions, and Recent Updates of EGFR Inhibitors. Current Topics in Medicinal Chemistry. 2020; 20: 815–834. https://doi.org/10.2174/1568026620666200303123102.
[44] Chu C, Huang Y, Ru Y, Lu X, Zeng X, Liu K, *et al*. α-MSH ameliorates corneal surface dysfunction in scopolamine-induced dry eye rats and human corneal epithelial cells via enhancing EGFR expression. Experimental Eye Research. 2021; 210: 108685. https://doi.org/10.1016/j.exer.2021.108685.
[45] Chen K, Li Y, Zhang X, Ullah R, Tong J, Shen Y. The role of the PI3K/AKT signalling pathway in the corneal epithelium: recent updates. Cell Death & Disease. 2022; 13: 513. https://doi.org/10.1038/s41419-022-04963-x.
[46] Craig JP, Nichols KK, Akpek EK, Caffery B, Dua HS, Joo CK, *et al*. TFOS DEWS II Definition and Classification Report. The Ocular Surface. 2017; 15: 276–283. https://doi.org/10.1016/j.jtos.2017.05.008.
[47] Jiang L, Sun S, Chen J, Sun Z. Random Forest Algorithm-Based Ultrasonic Image in the Diagnosis of Patients with Dry Eye Syndrome and Its Relationship with Tear Osmotic Pressure. Computational and Mathematical Methods in Medicine. 2022; 2022: 9437468. https://doi.org/10.1155/2022/9437468.
[48] Lian L, Ye X, Wang Z, Li J, Wang J, Chen L, *et al*. Hyperosmotic stress-induced NLRP3 inflammasome activation via the mechanosensitive PIEZO1 channel in dry eye corneal epithelium. The Ocular Surface. 2025; 36: 106–118. https://doi.org/10.1016/j.jtos.2025.01.005.
[49] Araki-Sasaki K, Ohashi Y, Sasabe T, Hayashi K, Watanabe H, Tano Y, *et al*. An SV40-immortalized human corneal epithelial cell line and its characterization. Investigative Ophthalmology & Visual Science. 1995; 36: 614–621.
[50] Yamasaki K, Kawasaki S, Young RD, Fukuoka H, Tanioka H, Nakatsukasa M, *et al*. Genomic aberrations and cellular heterogeneity in SV40-immortalized human corneal epithelial cells. Investigative Ophthalmology & Visual Science. 2009; 50: 604–613. https://doi.org/10.1167/iovs.08-2239.